# OBJECT-BASED BUILDING EXTRACTION IN TACNA, PERU USING WORLDVIEW-2 IMAGES

Kentaro Suzuki[1*], Wen Liu[2], Miguel Estrada[3], and Fumio Yamazaki[1]

1 Chiba University, 1-33, Yayoi-cho, Inage-ku, Chiba, 263-8522, Japan, kentaro_suzuki@chiba-u.jp; fumio.yamazaki@faculty.chiba-u.jp
2 Tokyo Institute of Technology, 4259-G3-2, Nagatsuta, Midori-ku, Yokohama 226-8502, Japan, liu.w.ad@m.titech.ac.jp
3 National University of Engineering, Av. Tupac Amaru 1150, Lima 25, Peru, estrada@uni.edu.pe

*Corresponding author: kentaro_suzuki@chiba-u.jp

## ABSTRACT

In conducting damage assessment for scenario earthquakes in high seismic risk regions, building inventory data are required as well as building fragility functions and strong-motion distributions. But inventory data with the locations and characteristics of buildings are not so easy to construct, especially for developing countries. Hence in this study, an approach to construct building inventory data is sought as an alternative of cadastral data and field surveys. Using a high-resolution optical satellite image acquired by WorldView-2, this paper tries to develop building inventory data for earthquake damage assessment in Tacna, Peru. First, Pixel-based classification was carried out to examine basic land-cover and land-use of the urban area. Object-based building extraction was then conducted for three selected areas as an attempt to develop building inventory data.

**Keywords**: object-based classification, WorldView-2, building extraction, damage assessment, building inventory

## INTRODUCTION

Building inventory data are necessary elements in seismic damage assessments, together with building fragility functions and strong-motion distributions. But inventory data with the locations and characteristics of buildings are not so easy to construct from the view point of labor and costs, for the countries with high disaster risks. A common practice to develop building inventory data is the use of cadastral (land tax register) data with supporting field validation. But cadastral data are not often prepared in the form to be used in earthquake damage assessment, especially in developing countries. Thus, GEM (Global Earthquake Model) Foundation [1] recently initiated a research project on Inventory Data Capture Tools (IDCT) to develop open source tools to generate information and models on building inventory from remote sensing [2, 3] and field observations [2].

Several very high-resolution (VHR) optical satellites with ground-resolution of 1 m or less have been launched and in operation in the last decade. Ikonos, the first commercial high-resolution satellite with maximum spatial resolution of 1.0 m, launched successfully on 25 September 1999, and QuickBird, with a maximum resolution of 0.6 m, launched on 18 October 2001, are the first generation of this category. GeoEye-1 (launched on 6 September, 2008) and WorldView-2 (launched on 8 October, 2009) with sub-meter ground-resolution are the second generation VHR satellites, succeeding Ikonos and QuickBird.

Using imagery data acquired from these satellite multispectral sensors, a number of studies on urban modeling and damage detection from natural disaster have been carried out in the various part of the world [4, 5]. For example, Miura and Midorikawa [6] updated existing building GIS data for earthquake damage assessment, using an Ikonos image in Metro Manila, the Philippines. They were able to extract mid- and high-rise buildings by image processing, but a land-cover classification map had to be employed to estimate the number of low-rise buildings in densely built-up areas. Sarabandi *et al.* [7] tried to extract building inventory information such as height, shape and square footage from single high-resolution remotely-sensed images for London, UK, using a new MIHEA (Mono Image Height Extraction Algorithm) tool. Marangoz *et al.* [8] extracted buildings at a cultural heritage site in

Turkey by pixel-based and object-based supervised classification from Ikonos imagery and pointed out that object-based classification got higher accuracy in building extraction than pixel-based classification did. Applications of object-based classification in extraction of intact and damaged buildings were tried for QuickBird images before and after the 2006 central Java, Indonesia earthquake [9] and for digital aerial images before and after the 2007 Mid-Niigata-Oki, Japan earthquake [10]. Object-based classification gave better results than pixel-based one for these VHR images, but still questions remain on the selection of bands and other spatial data, and the determination of parameter values in object-based approach.

In this study, as a first step to develop building inventory for earthquake damage assessment, object-based building extraction was conducted from a WorldView-2 image of Tacna City in the southern Peru. Pixel-based supervised classification was firstly applied to the whole city areas of Tacna to grasp overall land-cover and land-use. Secondly, based on the ratio of vegetation land-cover estimated from the classification and the population density from census data in each city-block, we chose three target areas for building extraction. Object-based supervised classification was then conducted for the target areas, and the result was discussed, comparing with that from visual inspection.

## SATREPS PROJECT AND STUDY AREA

As one of research projects under the framework of "Science and Technology Research Partnership for Sustainable Development (SATREPS [11])", under the joint sponsorship of Japan Science and Technology Agency (JST) and Japan International Cooperation Agency (JICA), a bilateral joint research project entitled "Enhancement of Earthquake and Tsunami Disaster Mitigation Technology in Peru" has been carried out by Japanese and Peruvian researches since 2009 [12]. The project aims comprehensive research on earthquake and tsunami disaster mitigation in five main research topics: 1) Strong motion prediction and development of seismic microzonation; 2) Development of tsunami countermeasures based on numerical simulation; 3) Enhancement of seismic resistance of buildings based on structural experiments and field investigations; 4) Development of spatial information databases using remote sensing technology and earthquake damage assessment for scenario earthquakes; 5) Development of earthquake and tsunami disaster mitigation plan and its implementation into society. Metropolitan Lima and Tacna City were selected as two case study areas after preliminary surveys. As a part of SATREPS Peru project, this paper investigates the methodology of building inventory data development for Tacna.

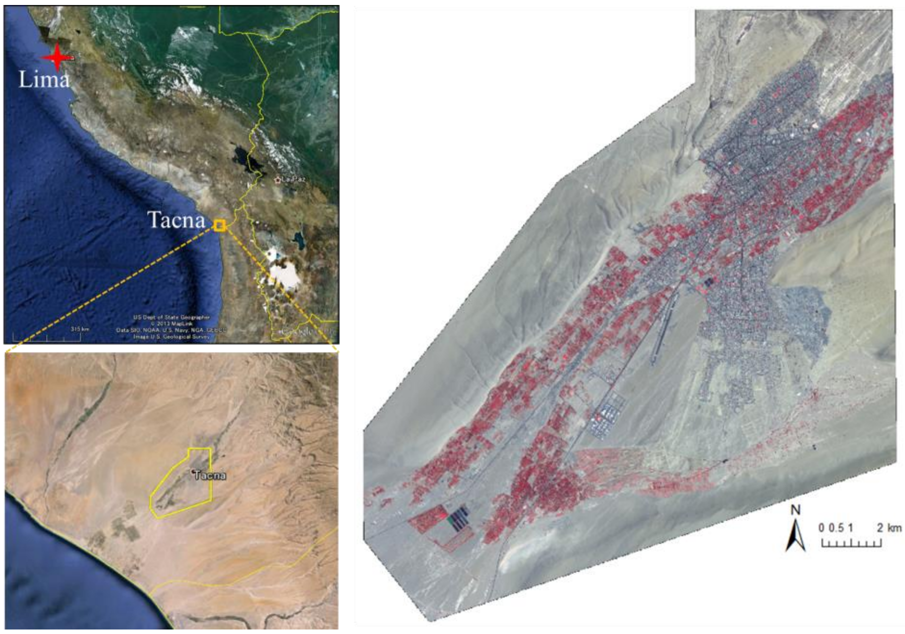


**Figure 1. The study area including Tacna in southern Peru and the imaging area, plotted on Google Earth (left), and the false color composite of WorldView-2 image (right)**

Scenario earthquake events for damage assessment for the project were determined based on recent studies [13, 14]. Two major historical earthquakes were selected for this purpose because these two events are the most damaging and are expected to have significant effects on Peru. The first event is the 1746 Lima-Callao earthquake (Mw 8.6) that destroyed the city of Lima completely and produced about 6,000 deaths. The second event is the 1868 southern Peru earthquake (Mw 8.8), which produced large tsunamis along the coasts of Peru and Chile. The earthquake almost completely destroyed Arica, Tacna, Moquegua and Arequipa areas, with about 25,000 deaths. The recurrence of these mega-earthquakes is anticipated along the Peru-Chile Pacific coast [15].

Tacna, the capital city of Tacna Region, is located in southern Peru, about 35 km north of the border with Chile, as shown in **Figure 1**. The city is in the valley of the Capina River, surrounded by desert and about 30 km inland from the Pacific Ocean. The city has the total population about 242,000 and its average elevation is 552 m.

A WorldView-2 (WV-2) image, shown in **Figure 1**, was taken on March 6, 2010 and the area of the image used in this study is shown with a yellow square. The resolution of the image is 0.5 m in the panchromatic (PAN) band and 2.0 m in the multispectral (MS) bands. Although the WV-2 sensor has 8 MS bands [16], the image we purchased is a bundle product of PAN and 4 MS (Blue, Green, Red, NIR-1) bands.

## LAND COVER CLASSIFICATION AND SELECTION OF TARGET EXTRACTION AREAS

In Peru, building inventory data have not been prepared as the use in damage assessment on a GIS platform. Hence, the construction of building inventory data is an important topic in disaster management research and practice. In conjunction with the SATREPS project, Estrada *et al.* [17] and Matsuoka *et al.* [18] have proposed methods to develop building inventory data from high-resolution satellite images (WV-2) together with some other geospatial data such as multi-temporal Landsat images, DEM, and census data. They demonstrated the method in Lima Metropolitan area and the results were compared with field survey data and visual inspection results of VHR images. But due to the shortage of ground truth data, validation is still necessary for practical applications. Thus we attempt a similar case study for Tacna to extract building inventory data from the VHR satellite image.

The extraction of buildings from an object-based analysis has to examine the most suitable parameters for different type of buildings (e.g., detached house, apartment building, factory) and their

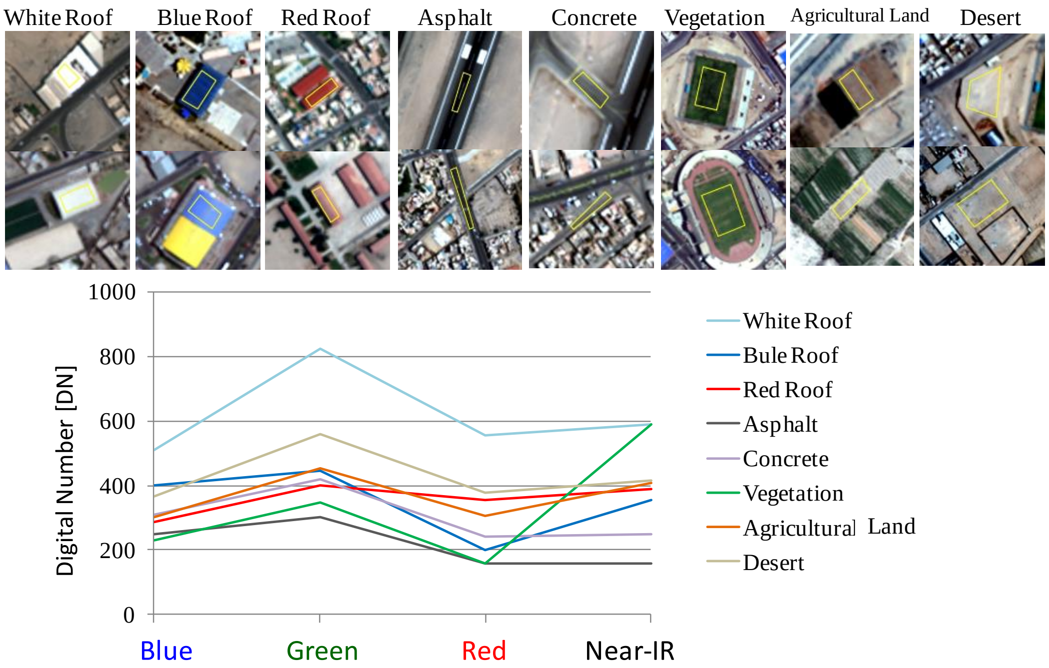


**Figure 2. Training data selected for the 8 land-cover classes and their mean DN values for the 4 MS bands of the WV-2 image**

surrounding condition (e.g., built-up density, vegetation, topography). Considering the spatial distribution of different type of buildings within Tacna City, land-cover classification was conducted for the WorldView-2 MS image to access general land-cover and land-use of the city.

As a first step, K-means unsupervised classification was attempted by changing the number of classes in order to determine the suitable land-cover classes in supervised classification. Considering the result from unsupervised classification, the maximum likelihood supervised classification was conducted using 8 land-cover classes (white roof, blue roof, red roof, asphalt, concrete, vegetation, agricultural land, desert). **Figure 2** shows the training data selected for the 8 classes and their mean digital numbers (DNs) for the 4 MS bands of the WV-2 data. The result of supervised classification is shown in **Figure 3 (a)**. The result shows the distribution of vegetation along the river clearly.

Then, the coverage ratio of vegetation class from the supervised classification within each city block was calculated and shown in **Figure 4 (a)**. From this figure, a ratio of vegetation is seen to be high in the city center and very low in the south of the city. Using the national census data [19], the population density for each city block was also calculated as shown in **Figure 4 (b)**. From the figure, many high-density blocks are seen in the northern part and many low-density blocks in the southern part of the city. From the combination of these two maps (vegetation and population density), the urban area of Tacna City can be divided into residential and commercial (or industrial) based on the population density, and then residential areas are further categorized into highly built-up residential and low-density residential based on vegetation.

From this observation, we assumed three typical land-use types in the city, 1) area with mostly large buildings of commercial/residential use or industrial use, 2) residence area with high vegetation ratio, and 3) high-density residential area with low vegetation ratio. Then three 300m x 300m target areas were extracted as shown in **Figure 3 (b)** for typical examples of the three land-use types, and they were used for more detailed building extraction by object-based classification.

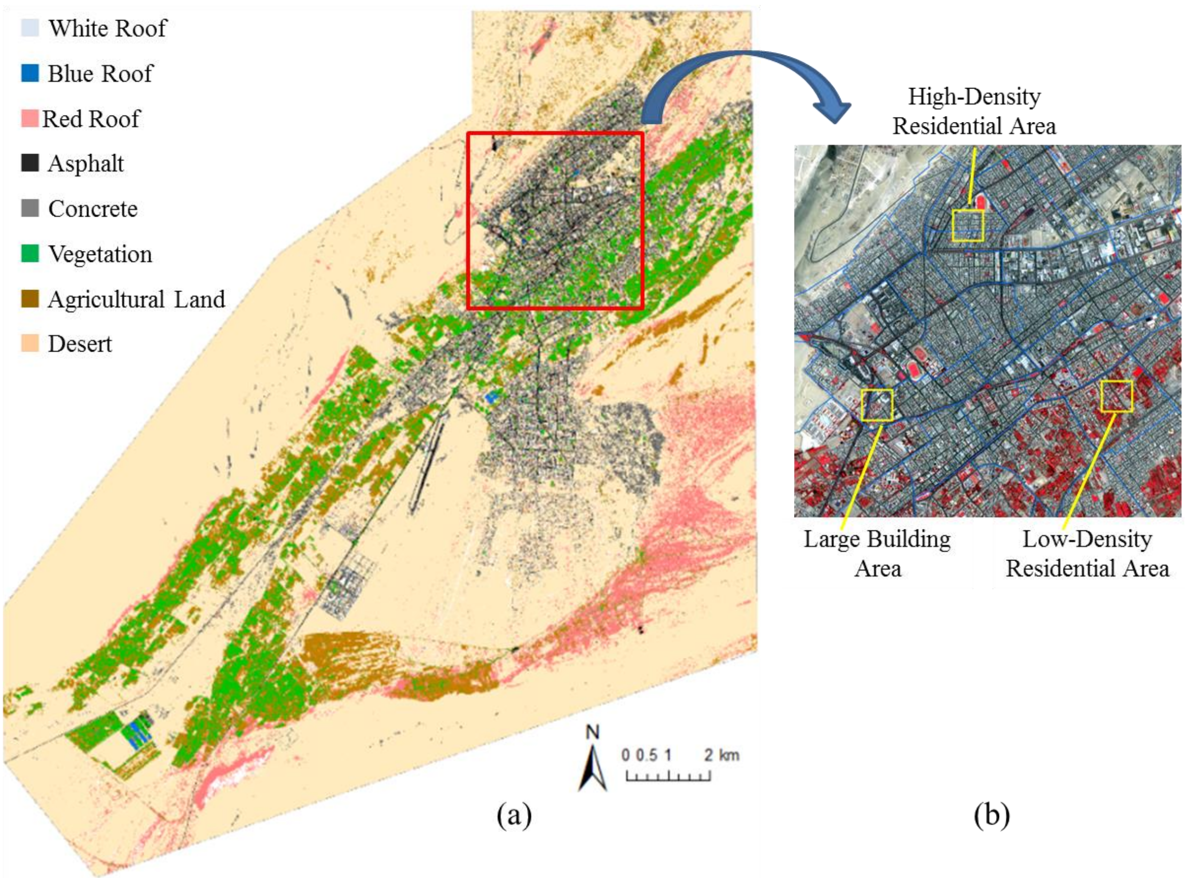


**Figure 3. The result of pixel-based supervised classification with 8 classes for the MS image (a) and the selected three target areas for detailed investigation (b)**

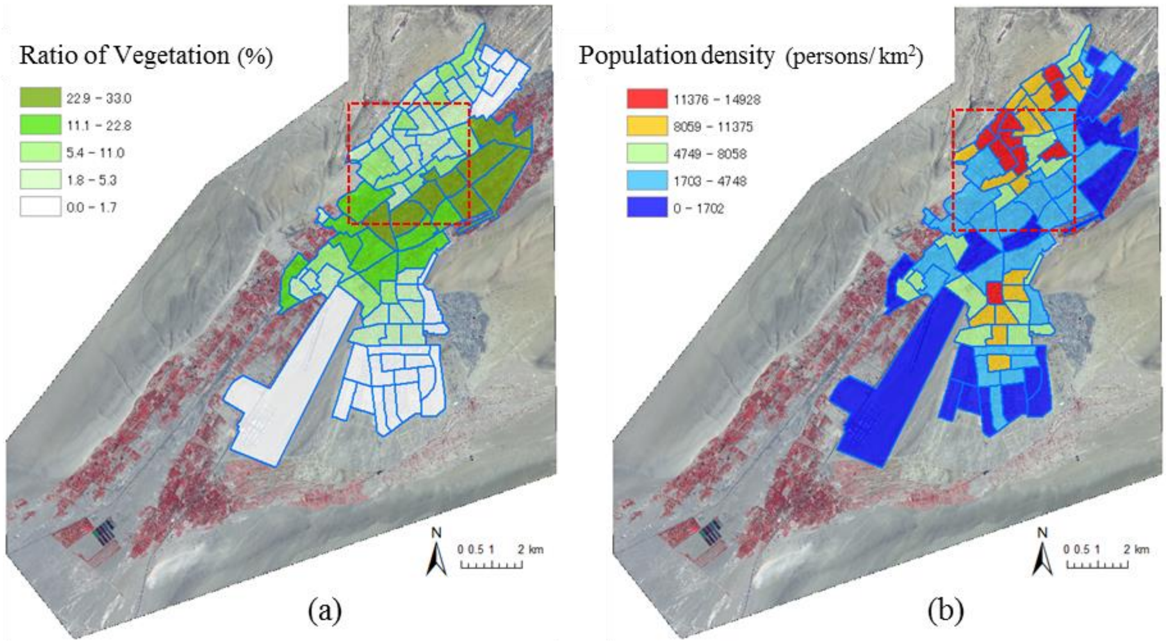


**Figure 4. (a) Ratio of vegetation obtained by pixel-based supervised classification and (b) population density obtained from national census data for each city block**

## SEGMENTATION AND OBJECT-BASED CLASSIFICATION

Definiens Professional 5 software was used in performing object-based classification. First, image segmentation was conducted to make "objects". The segmentation process is determined by 5 parameters: *Layer Weight*, *Compact Weight*, *Smooth Weight*, *Shape Factor*, and *Scale Parameter*. Since *Scale Parameter* determines the object size, it is changed depending on the size of buildings to pay attention to. In this study, *Scale Parameter* is determined as 150, 100, 80 for the large building, low-density residential, and high-density residential areas, respectively. *Shape Factor* determines the importance level of spectral heterogeneity or shape heterogeneity in segmentation. When the shape factor moves toward 0, spectral heterogeneity is more concerned. On the contrary, if it moves toward 0.9, shape heterogeneity is more concerned. In this study *Shape Factor* was determined as 0.9 in order to extract building edges. In further details, the spectral heterogeneity is decided by *Layer Weight*, which gives the weight for each band. It is assumes as 1.0 for each band here. The shape heterogeneity is decided by *Compact Weight* and *Smooth Weight*. Bigger *Compact Weight* indicates that the segmented objects are in more compact shape. Alternatively, bigger *Smooth Weight* shows that the segmented objects are in more smooth shape. *Compact Weight* and *Smooth Weight* were determined as 0 and 1.0, respectively since the outlines of buildings are linear. The result of segmentation is shown **Figure 5** (left). Because of the selection of proper values for Scale Parameter, the results of segmentation for buildings are seen to be reasonable.

Next, Nearest-Neighbor (NN) supervised classification was conducted for the objects created by the segmentation step. The number of classes for the large building area (a) and the high-density residential area (c) is 7 while that for the low-density residential area (b) is 8, by adding "Water" class. The result of object-based classification is shown **Figure 5** (center). In area (a), apartment buildings and factories with uniform roof-color were classified correctly. However, a basketball court whose color is similar to that of blue-roof was misclassified. In area (b), the outlines of buildings could not be extracted so well, but the locations of buildings could be estimated from the objects classified as building roofs. In area (c), since building roofs are located very close one another with complicated shapes and colors, the extraction of building outlines was difficult by object-based classification and even by manual interpretation. Thus, instead of extracting individual buildings, the extraction of blocks surrounded by roads may be more suitable in high-density areas. The number of buildings in each block can be estimated through field surveys and census/cadastral data.

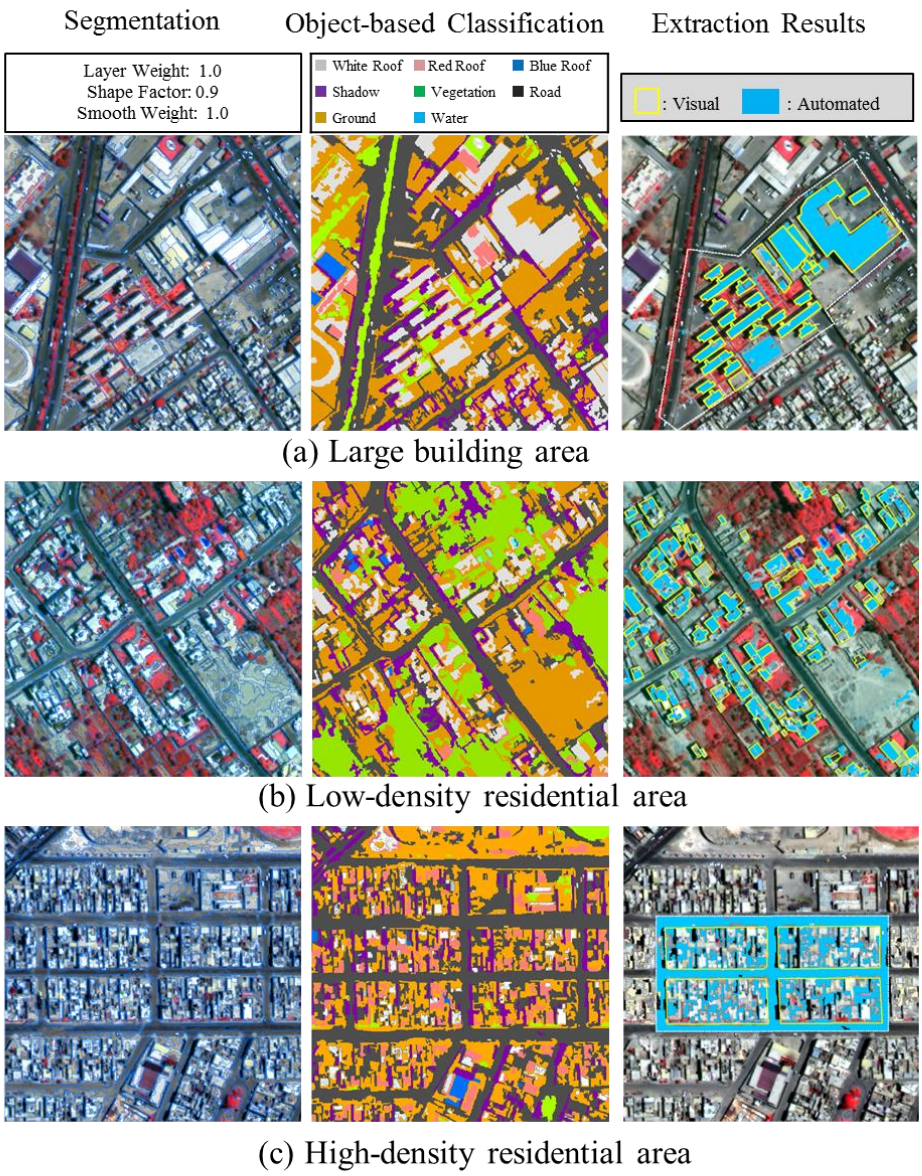


**Figure 5. Result of segmentation (left), object-based classification (center), and extracted regions and building outline made manually (right) for the three target areas**

**BUILDING EXTRACTION AND EVALUATION OF ACCURACY**

In order to perform quantitative evaluation on the accuracy of building extraction, building footprints were drawn manually for the large building and low-density residential areas and city-blocks surrounded by roads were drawn manually in **Figure 5** (right) together with the extracted roof objects by object-based classification. The accuracy of building extraction is measured by comparing the areas covered by buildings (city blocks in the high-density residential area) or other materials in the truth data and the supervised classification results, shown in **Tables 1-3**. The user accuracy represents the correct answer rate that the area extracted by object-based classification overlaps with the area extracted manually, and the producer accuracy shows the ratio how much area extracted manually was extracted by object-based classification.

In the large building area, the user accuracy was very high as 87.6% for buildings. The user accuracy was also high as 75.7%. Hence the accuracy of object-based classification is considered to be high if buildings are large enough, compared with the image resolution and they are standing alone surrounded by open space. In the low-density residential area, the producer accuracy for buildings was low (47.6%) while the user accuracy was rather high (75.2%). This indicates that many houses were

**Table 1. Error matrix of extraction for the large building area**

| | | Visual Inspection ($m^2$) | | | User's Accuracy |
|---|---|---|---|---|---|
| | | Building | Others | Sum | |
| Extraction Result ($m^2$) | Building | 7874 | 1112 | 8986 | 87.6 % |
| | Others | 2526 | 19818 | 22344 | 88.7 % |
| | Sum | 10400 | 20930 | 31330 | |
| Producer's Accuracy | | 75.7 % | 94.7 % | Overall Accuracy | 88.4 % |

**Table 2. Error matrix of extraction for the low-density residential area**

| | | Visual Inspection ($m^2$) | | | User's Accuracy |
|---|---|---|---|---|---|
| | | Building | Others | Sum | |
| Extraction Result ($m^2$) | Building | 6904 | 2274 | 9179 | 75.2 % |
| | Others | 7608 | 73213 | 80821 | 90.6 % |
| | Sum | 14512 | 75488 | 90000 | |
| Producer's Accuracy | | 47.6 % | 97.0 % | Overall Accuracy | 89.0 % |

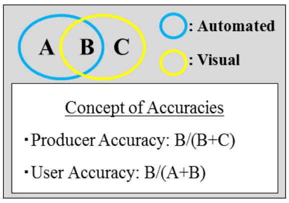


**Table 3. Error matrix of extraction for the high-density residential area**

| | | Visual Inspection ($m^2$) | | | User's Accuracy |
|---|---|---|---|---|---|
| | | Building Block | Road | Sum | |
| Extraction Result ($m^2$) | Building Block | 12435 | 1456 | 13891 | 89.5% |
| | Road | 5771 | 8253 | 14024 | 58.8% |
| | Sum | 18206 | 9708 | 27915 | |
| Producer's Accuracy | | 68.3% | 85.0% | Overall Accuracy | 74.1% |

classified as other classes because roof colors and materials in the area had wide variation, including those similar to road and ground.

In the high-density residential area, the user accuracy for block extraction is as high as 89.5%, but the producer accuracy was not so high (68.3%). This example shows the difficulty in the extraction of buildings in densely built-up areas, even in a block level. The extraction method for roads may ease this difficulty somewhat.

## CONCLUSION

Building inventory data are necessary in conducting damage assessment for scenario earthquakes in high seismic risk regions. But such inventory data with the locations and characteristics of buildings are not so easy to construct, especially for developing countries. Hence in this study, an approach to construct building inventory data is sought using a high-resolution optical satellite image acquired by WorldView-2, covering Tacna in southern Peru. First, pixel-based classification was carried for the multispectrum (MS) image in order to examine basic land-cover and land-use of the urban area. From this analysis, a ratio of vegetation-class land-cover in each city-block was evaluated as well as other land-cover classes. Together with the population density evaluated from census data, the characteristics of the whole city area were evaluated in terms of vegetation and pupulation density. Three areas were selected such as 1) Area with large buildings, 2) Low-density residential, and 3) High-density residential. By selecting 300m x 300m small areas representing the three land-use types, object-based classification was carried out. Image segmentation was conducted first considering the size of buildings in each area. The object-based supervised classification was then carried out for the segmentation results, and the classification results were compared with manually produced building footprints for area types-1 and -2, and city-blocks for area type-3. The error matrices for the three areas showed that extraction of indivisual buildings has high accuracy for Areas 1 and 2, but the extraction of blocks sometimes falls in difficulty for Area 3. Since this paper provided only preliminary examination, a more comprehensive study is now on going.

**REFERENCES**

[1] GEM Foundation, Available online: http://www.globalquakemodel.org/, (accessed on 15th September 2013).
[2] Inventory Capture Tools, Available online: http://www.globalquakemodel.org/what/physical-integrated-risk/inventory-capture-tools/, (accessed on 15th September 2013).
[3] Wieland M., Pittore M., Parolai S., Zschau J., 2012, Remote sensing and omnidirectional imaging for efficient building inventory data-capturing: Application within the Earthquake Model Central Asia, *2012 IEEE International Geoscience and Remote Sensing Symposium*, 3010 - 3013.
[4] Rathje E., and Adams B.J., 2008, The role of remote sensing in earthquake science and engineering, opportunities and challenges, *Earthquake Spectra*, 24(2) 471–492.
[5] Eguchi R.T., Huyck C., Ghosh S., Adams B.J., 2008, The application of remote sensing technologies for disaster management, *The 14th World Conference on Earthquake Engineering*, CD-ROM, 17.
[6] Miura H., and Midorikawa S., 2006, Updating GIS building inventory data using high-resolution satellite images for earthquake damage assessment: application to metro Manila, Philippines, *Earthquake Spectra*, 22(1) 151-168.
[7] Sarabandi P., Chung H-C., and Adams B.J., 2006, Remote sensing for building inventory updates in disaster management, *Proc. of SPIE*, (6178) 10. Available online: http://proceedings.spiedigitallibrary.org/, (accessed on 15th September 2013).
[8] Marangoz A. M., Oruç M., Karakış S., Şahin H., 2006, Comparison of pixel-based and object-oriented classification using IKONOS imagery for automatic building extraction–Safranbolu testfield, *Fifth International Symposium "Turkish-German Joint Geodetic Days"*, Berlin Technical University, 28-31.
[9] Matsumoto K., Vu T.T., and Yamazaki F., 2006, Extraction of damaged buildings using high resolution satellite images in the 2006 central Java earthquake, *Proc. 27th Asian Conference on Remote Sensing*, CD-ROM, 6.
[10] Suzuki D., and Yamazaki F., 2008, Extraction of building damages in the 2007 Niigata-Ken Chuetsu-Oki earthquake using digital aerial images, *Proc. 29th Asian Conference on Remote Sensing*, Paper No. 156, CD-ROM, 6.
[11] Japan Science and Technology Agency (JST), SATREPS, Available online: http://www.jst.go.jp/global/english/index.html, (accessed on 15th September 2013).
[12] Yamazaki, F. and Zavala, C., 2013, SATREPS project on enhancement of earthquake and tsunami disaster mitigation technology in Peru, *Journal of Disaster Research*, 8(2), 224-234.
[13] Sladen A., Tavera H., Simons M., Avouac J. P., Konca A. O., Perfettini H., Audin L., Fielding E. J., Ortega F., and Cavagnoud R., 2010, Source model of the 2007 Mw 8.0 Pisco, Peru earthquake: Implications for seismogenic behavior of subduction megathrusts, *Journal of Geophysical Research*, 115, B02405.
[14] Pulido N., Tavera H., Aguilar Z., Chlieh M., Calderon D., Nakai S., Sekiguchi T., Yamazaki F., 2012, Mega-earthquakes Rupture Scenarios and Strong Motion Simulations for Central Andes, Peru, *The International Symposium for CISMID 25th Anniversary*, Lima, Peru, CD-ROM, Paper No. TS-6-2, 8.
[15] Okal, E.A., Borrero, J.C., and Synolakis, C.E., 2006, Evaluation of Tsunami Risk from Regional Earthquakes at Pisco, Peru, *Bulletin of the Seismological Society of America*, 96(5), 1634–1648.
[16] DigitalGlobe, Inc., 2010, Radiometric Use of WorldView-2 Imagery: Technical Note, Available online:http://www.digitalglobe.com/sites/default/files/Radiometric_Use_of_WorldView-2_Imagery%20(1).pdf, (accessed on 14th September 2013).
[17] Estrada M., Miura H., Yamazaki F., and Midorikawa S., 2011, Land use evaluation using satellite imagery for urban inventories, *8th International Conference on Urban Earthquake Engineering*, Tokyo Institute of Technology, 93-96.
[18] Matsuoka M., Miura H., Midorikawa S., and Estrada M., 2013, Extraction of urban information for seismic hazard and risk assessment in Lima, Peru using satellite imagery, *Journal of Disaster Research*, 8(2), 328-345.
[19] PERU Instituto Nacional de Estadística e Informática INEI, Available online: http://www.inei.gob.pe/, (accessed on 15th September 2013).